Article ID: 1006-8775(2016) 02-0233-10

CLIMATOLOGICAL CHARACTERISTICS OF SPRING PRECIPITATION OVER SOUTHERN CHINA AND ITS INTRASEASONAL OSCILLATION

PAN Wei-juan (潘蔚娟)[1], LI Chun-hui (李春晖)[2], JIANG Cheng-lin (蒋承霖)[3]

(1. Guangzhou Climate and Agrometeorology Center, Guangzhou Meteorological Administration, Guangzhou 511430 China; 2. Institute of Tropical and Marine Meteorology/Guangdong Provincial Key Laboratory of Regional Numerical Weather Prediction, CMA, Guangzhou 510080 China; 3. Guangdong Provincial Climate Center, Guangzhou 510080 China)

Abstract: Based on observations and reanalysis data, the characteristics of the evolution of climatological spring precipitation over Southern China (SPSC) and the associated climatological intraseasonal oscillation (CISO) and atmospheric circulation are studied. Results show that SPSC increases in an oscillatory way. Although the evolution of SPSC is similar in different regions, there are also differences. In different regions of Southern China, the onset dates of the rain season are from the 12th to 24th pentad and the peak dates are after the 20th pentad. CISO is an important component of SPSC, which is not only statistically significant, but also accompanies a dynamically coherent structure. The peak wet/dry phase of each CISO cycle corresponds to a significant rainfall increasing/decreasing period and modulates the evolution of SPSC. The rainfall growth in the second half of March and mid-April is the result of the modulation. The wet/dry phase of CISO is accompanied by low-level convergent (upper-level divergent) and cyclonic (anti-cyclonic) circulation, which favors ascending motion to develop over Southern China.

Key words: spring precipitation over Southern China; wavelet analysis; climatological intraseasonal oscillation
CLC number: P462.4 **Document code:** A
doi: 10.16555/j.1006-8775.2016.02.013

1 INTRODUCTION

A lot of studies on seasonal shifts have pointed out that spring precipitation in Southern China and areas to the south of the Yangtze occurs before seasonal precipitation and has important effect on the subsequent onset of the summer monsoon and the progression of seasonal precipitation in China. The beginning and ending dates, nature, mechanisms for the formation, influencing factors and associated circulation patterns have been receiving increasing attention (Gao et al.[1]; Bao[2]; Tien and Yasunari[3]; Chen et al.[4]; Liang and Wu[5]; Wang et al.[6]; Qian et al.[7]; Wang and LinHo [8]; Chi [9]; Wan and Wu[10]; Zhao et al.[11]; Wang and Ding[12]; Wan and Wu[13]; Wan et al.[14]; He et al.[15]; LinHo et al.[16]; Zhu et al.[17]). The precipitation of interest covers a vast region comprising the above two regions but it is abbreviated, for the ease of discussion, as spring precipitation over Southern China (SPSC). According to Wan et al.[13, 14], this rain covers an area south of 30°N, east of 110°E and north of Leizhou Peninsula and lasts between 13 and 27 pentads. SPSC is a typical synoptic phenomenon that is present during the transition from winter to spring in East Asia, which corresponds to a series of change in the atmospheric circulation[16]. As far as the interannual variation, the SPSC is mainly correlated with the anomalous circulation in the northern Pacific and the part of the general circulation linked with it is not similar to the summer monsoon or winter monsoon circulation, showing the complicated nature of the systems governing it[6]. As the initial phase of the rain season in Southern China, the start of the spring rain and its progression indicate the change from a dry winter pattern of climate to a rainy season, a longtime focus of attention for flood and drought mitigation. Previous studies work on the progress of SPSC by treating the Southern China as a whole while doing little in comparing the regional difference.

Using climatologically averaged daily data, Nakazawa[18] concluded that the convection in the Indian Ocean and West Pacific enhances intermittently at periods of 30-60 d during the Asian summer monsoon and shows significant seasonal phase-lock. From the viewpoint of statistical significance and dynamic coordination, Wang and Xu[19] studied the climatological intrasea-

Received 2014-10-31; **Revised** 2016-02-25; **Accepted** 2016-04-15
Foundation item: National Program for Key Fundamental Research and Development (2012CB417205); International Cooperation Project for Ministry of Science and Technology (2009DFA23010); National Project for Science and Technology Support (2009BAC51B); Project of Science and Technology for Guangdong Province (Meteorological Sector) (200905); National Natural Science Foundation of China(41205069)
Biography: PAN Wei-juan, Ph.D., Associate Researcher, primarily undertaking research on short-range climate prediction and operation of climate monitoring and diagnosis.
Corresponding author: PAN Wei-juan, e-mail: wjpan@grmc.gov.cn

sonal oscillation (CISO), a component in the summer monsoon in Northern Hemisphere, and argued that CISO is a component of the intraseasonal phase-lock in the annual cycle with the phase of extreme values corresponding to the singular point of the shifting process of the summer monsoon. According to Wang and Ding[12], CISO significantly modulates the intensity of the rain season in Eastern China and may be an internal mechanism that restrains the onset, enhancing, weakening and re-enhancing of seasonal rain bands apart from increasing the amplitude of precipitation. Is there also significant CISO with the SPSC? If yes, does it have similar phase-locking effect and modulating role? How does its associated intraseasonal oscillation behave in the atmospheric circulation? Work is little on this aspect. Climatologically, this study discusses the SPSC in terms of its onset and progression in various parts of Southern China and studies the significance of CISO and its associated features of the atmospheric circulation.

2 DATA AND METHODOLOGY

Daily precipitation data from 177 observation stations in the area east of 105°E and within 20°-32°N for 1980-2008 (29 years) are used to run the following two types of processing. (1) Take 5 d as a pentad and average the rainfall of each of the stations on a yearly and pentad basis to determine the daily mean rainfall (shortened as pentad averaged rainfall) climatologically averaged (on the basis of years, the same hereafter) for 73 pentads. (2) The daily rainfall for every spring (March to May, or a total of 92 d) of each of the stations is processed with 5-d running mean to filter out synoptic disturbances to determine daily rainfall of 5-d running mean that is climatologically averaged over spring.

For this study, the wind field and temperature are extracted from the reanalysis dataset of ERA-Interim from European Center for Medium-Range Weather Forecast (Dee et al.[20]) for the 20 years of 1989-2008 with a horizontal resolution of 0.5°×0.5°. Employing the same technique as with the rainfall data, daily wind field and temperature processed with 5-d running mean are obtained and on the basis of that, climatologically averaged diversity and vorticity are known.

2.1 *CISO and wavelet analysis*

Wang and Xu[19] decomposed a climatological mean series into three parts: $y_c=y_{ca}+y_{ciso}+R(i)$, in which y_{ca} is the component of the annual cycle, y_{ciso} that of CISO and $R(i)$ that of climatological high-frequency oscillation.

As an efficient way of time frequency analysis (Torrence and Compo [21]), the wavelet transform has been widely used in signal identification. In this work, the Daubechies (DB) wavelet with a vanishing moment of 16 (DB16, see Cohen et al.[22]) is used. With the method of multiresolution, a preliminary series with a length of 92 (e.g. daily mean rainfall and wind for March to May) is decomposed into components made up of six frequency bands, which include a low-frequency component ($a0$, with a quasi-period >47.2 d) and five high-frequency components ($d1$ to $d5$, with quasi-periods at 47.2, 23.6, 11.8, 6.0 and 3.0 d). $a0$ is actually the signal of the annual cycle, the sum of components $d1$, $d2$ and $d3$ is the signal of CISO and $d5$ and $d6$ are the components of climatological high-frequency oscillation. Two variables, the wavelet energy spectrum and the signal of dominating anomaly, are separately used to conduct significance tests on the amplitude and frequency of the phase with extreme CISO values.

2.1.1 CRITERIA FOR VERIFYING THE WAVELET ENERGY SPECTRUM

Using the Monte Carlo method (Robert et al.[23]), the criteria for verifying the 5% significance are determined through computation: First, 29 random series are selected to obtain a 29-year mean series (with a length of 92) that has been processed with 5-d running mean, wavelet reconstruction is done after the series is standardized, and the wavelet energy spectrum is derived for the components of each of the frequency bands. Then, repeat the computation above for 1 000 times to rank the results in a decreasing order and the 50th value is taken as the standard to test the 5% significance level (Table 1). When the verified daily rainfall series is standardized and the value of the energy spectrum obtained through wavelet reconstruction differs from the corresponding threshold by values larger than 0, the amplitude of the CISO component is considered to be statistically significant at the 5% significance level.

Table 1. Parameters of the wavelet analysis.

Component	Quasi-period/d	Threshold of 5% significance for wavelet energy spectrum
$a0$	>47.2	0.30
$d1$	47.2	0.30
$d2$	23.6	0.45
$d3$	11.8	0.51
$d4$	6.0	0.15
$d5$	3.0	0.14
CISO	10~90	0.86

2.1.2 THRESHOLDS FOR VERIFYING THE SIGNAL OF DOMINANT ANOMALY

Following the method in Wang and Xu[19], the threshold of significance test is derived for the signal of dominant anomaly. The Bernoulli trial is a repetitive and in dependent test. Assuming that only two reciprocal results, A and $\overline{A}$, can occur in each test by probabilities of p and q, then A appears for r times in n tests by a probability (Tu et al.[24]) of

$$p(r)=C_n^r p^r q^{n-r} \quad (r=0,1,\cdots\cdots,n) \tag{1}$$

Next, the CISO components (i.e. the sum of $d1$, $d2$ and $d3$) are reconstructed for the wavelet of 5-d running mean daily rainfall for every spring in 1980-2008. With the assumption that in a given day the CISO shows pos

itive or negative anomaly by a probability of 50%, Eq. (1) is used to determine that there are 18 years in which the probability is about 7% for this day to be positive (negative). In other words, for the 29 years, when the number of years in which the CISO shows positive anomaly in a given day is more than 17 or less than 12, the dominance for the anomaly sign of that day is statistically significant on the 7% significance level. Therefore, I_{sgn}, the sign of a dominant anomaly, is defined as:

$$I_{\mathrm{sgn}}=\begin{cases} n-17 & (n>17) \\ n-12 & (n<12) \\ 0 & (12\le n\ge 17) \end{cases} \quad (2)$$

where n is the number of years in which the CISO shows positive anomaly on a given day. During the analysis, when $I_{sgn}\geqslant 1$ (or $I_{sgn}\leqslant$-1) on a given day, the sign of the positive (negative) dominant anomaly is statistically significant, i.e. that day is the singular point of a significant wet (dry) phase.

2.2 *Effective degrees of freedom and the filter series*

As the degree of autocorrelation increases and the degree of freedom decreases with running mean or filtering, effective degrees of freedom need to be known to derive corresponding thresholds of significance tests when undertaking significance tests of the correlation coefficient of a given series of X and Y. In this work, a method proposed by Chen[25] is used in computing the effective degrees of freedom.

2.3 *Correlation vector*

To discuss the correlation between the wind field and a given variable, R, the vector of correlation, is defined in a manner put forward by Wen and Zhang[26]:

$$R=R_u i+R_v j \quad (3)$$

where R_u and R_v are the coefficients of correlation between a given variable and the zonal wind u and meridional wind v, respectively. For the ease of discussion, the correlation vector is described directly by wind direction, for instance, the meridional (zonal) positive correlation vector is called the southerly (westerly) wind. To test the statistical significance of $|R|$, the threshold is determined depending on the degree of effective freedom.

2.4 *Onset dates of the rain season and maximum pentad-averaged rainfall*

Following the definition of deep convective precipitation (6 mm/d) as presented in Qian et al.[7], the first pentad in which the rainfall larger than 6 mm/d is defined to be the starting date of a rain season. Besides, the maximum mean rainfall for each of Pentads 13-27 is defined as the maximum pentad-mean rainfall in spring.

3 CLIMATOLOGY OF THE START AND PROGRESSION OF SPSC

Following Wan and Wu [13], Pentads 13-27 are chosen as the period of time for spring precipitation. Fig.1a gives the distribution of climatologically averaged total rainfall over these pentads. The rainfall is greater than 300 mm in the area east of 110°E and south of 30°N and there are two large-value centers in Fogang and Qingyuan (south of Nanling Mountains) and Wuyi Mountains with rainfall above 550 mm. Such distribution of the location and intensity of rainband centers result from the orographic effect of the two mountain ranges[13]. It is noteworthy that there are areas of relatively small amount of rainfall in southwestern Jiangxi and southern Hunan. As shown in Fig.1b, the southerly airflow meets the northerly one over Southern China at 850 hPa during this time and the South China Sea region is dominated by anti-cyclonic circulation in which a southwesterly flow diverted on the northwest side converges with the southwesterly flow from the Indochina Peninsula, making a warm and humid southwesterly a dominant flow for the Beibu Bay and Guangxi-Guangdong area. During the time, positive vertical vorticity is large (higher than 0.5×10^{-5} s^{-1}) over Southern

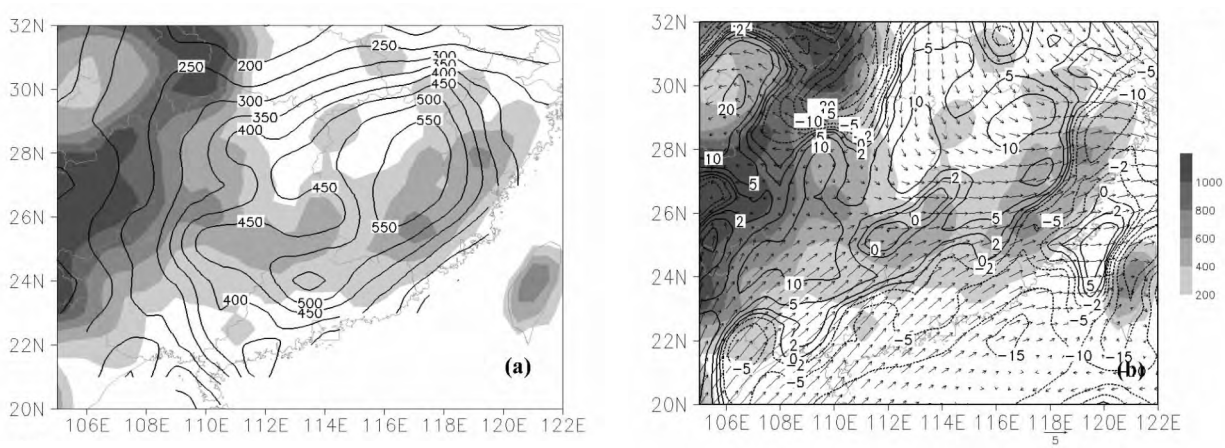

Figure 1. (a) Total rainfall (unit: mm) and (b) 850-hPa wind (vector, unit: m/s) and vertical vorticity (contours, unit: 10^{-6} s^{-1}) for climatologically averaged Pentads 13-27. The shades are for altitude of terrain in the unit of m.

China but small or even replaced with negative vorticity in southwestern Jiangxi and southern Hunan. The vorticity is also relatively small, and even forms a negative center, on the pentad basis (figure omitted). The center is located west of the southern section of Luoxiao Mountains and north of the Mengzhu Summit and Qitian Summit of Nanling Mountains, which should reflect the effect of leeside terrain (Smith[27]; Lin[28]).

It is shown in Fig.2 that the rain season starts at much different time across Southern China. It starts from the center of large rainfall amount and then pushes outwards. At around Pentad 12, it commences first from eastern Jiangxi and western Fujian, a result that is consistent with the observation that SPSC begins at Pentad 12 or 13 [3, 13]. At Pentad 15, the rain season spreads to Fujian and most of Jiangxi as well as northern Guangdong, and at Pentad 18, it expands to Zhejiang, southern Anhui, central and eastern Hunan and central Guangdong. Pentad 24 is the time when central and eastern Guangxi and western Jiangxi witness the beginning of the rain season. In contrast, it starts at a relatively late time in southwestern Jiangxi and southern Hunan.

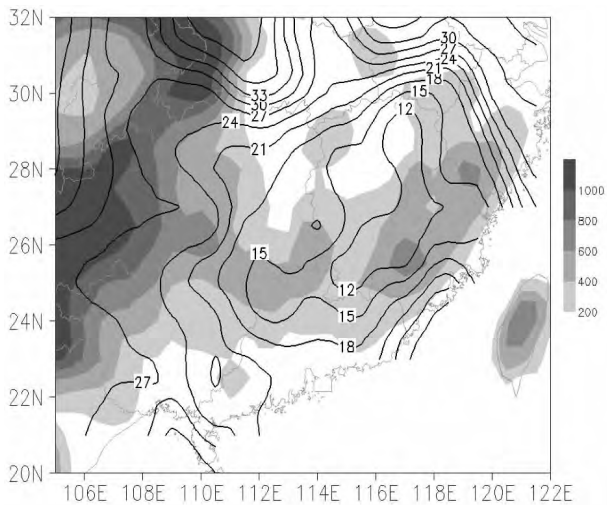

Figure 2. Time of spring precipitation occurrence in different parts of Southern China. Unit: pentad. The shades indicate the terrain altitude in the unit of m.

Figure 3a gives the distribution of maximum pentad-mean rainfall during the spring precipitation. The rain rate is above 7 mm/d in the area east of 108°E and south of 30°N. There are two large-value centres larger than 10 mm/d, one being consistent with the center of total rainfall in the Wuyi Mountains and the other being in the central and western Guangdong and central and eastern Guangxi. In the time of appearance (as shown in Fig.3b), maximum rainfall is first observed around Pentad 20 in the area adjoining Guangdong, Hunan and Jiangxi, the central and southern part of China, and the area of southern Jiangxi and part of western Fujian, with the surrounding areas phasing into the prime time of spring precipitation later.

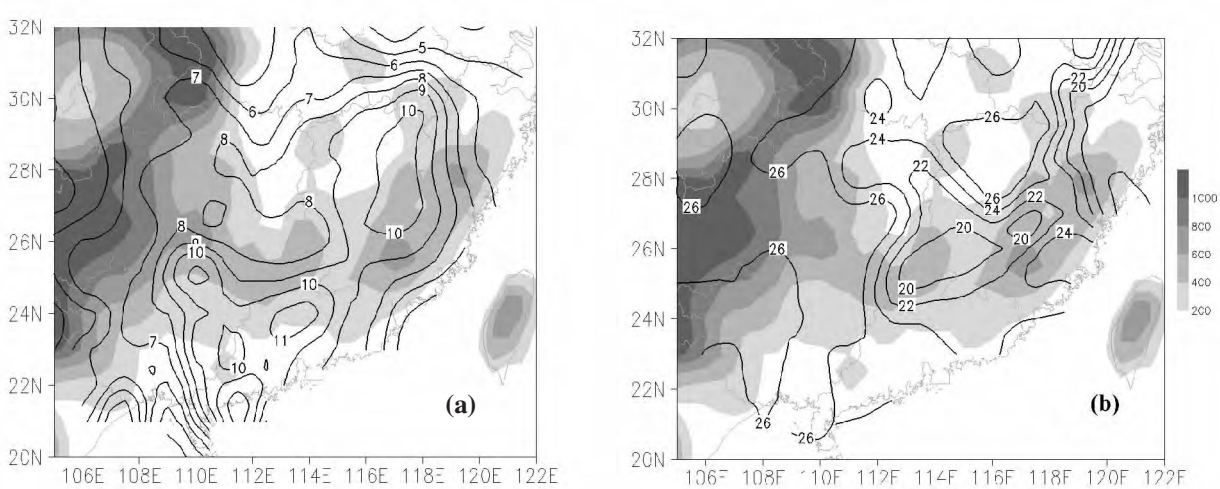

Figure 3. Maximum pentad-mean rainfall (a, the contour, unit: mm/d) and time of occurrence (b, the contour, unit: pentad) during the spring precipitation (Pentads 13-27). The shades indicate the terrain altitude in the unit of m.

Figure 4 gives the latitude-time evolution of daily rainfall averaged over 110°-120°E. It is shown that rainfall increases gradually with time but in different processes of development in the southern and northern part of Southern China. For the area between 23°-30°N, precipitation increases significantly in the latter half of March, from 6 to 8 mm, it increases by large margin, again, from early April to mid-April, with the peak appearing towards the middle of the month, about 10 mm, before the intensity drops slightly afterwards, and another peak occurs in mid-May. A center of precipitation pushes to the south from mid-March to early May, which not only shows signs of seasonal growth but also oscillations on the intraseasonal scale.

As shown in the analysis presented above, Pentad 12 is the time when parts of Southern China step into the rain season and rainfall is increasing gradually afterwards. After Pentad 20, they are all in the prime time of the rain season. The setup, enhancement and maintenance of SPSC result from the strengthening of a southwesterly wind, the increasing of cyclonic vorticity and water vapor convergence and the development of the vertical motion in Southern China, and are closely linked with the increasing of sensible heating over the bulk and southeastern part of the Tibetan Plateau and the East Asian continent and the reversal of zonal thermal contrast between the East Asian continent and the West Pacific[11, 13, 15]. Besides, the development of a main vortex in Southwestern China and the West Pacific subtropical high help strengthen the southwesterly wind[11]. By Pentad 13, the velocity of the southwesterly wind and rainfall of the SPSC have upgraded to a new level before strengthening further afterwards[13]. By Pentad 16, a channel has formed that transports water vapor from the West Pacific to Southern China and convergence in the front of the channel causes the rainfall to increase significantly in Southern China and area to the south of the Yangtze River[15].

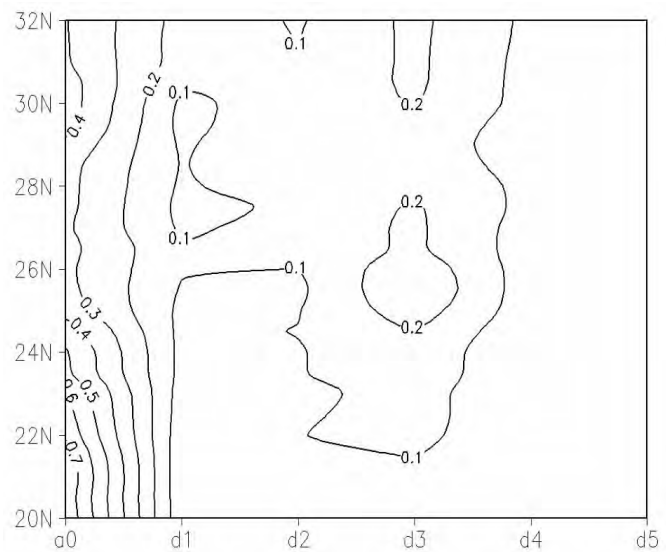

Figure 4. Zonal distribution of six wavelet-reconstructed components and variance ratio of the primitive series of the daily rainfall of the spring precipitation averaged over 110°-120°E.

4 CHARACTERISTICS OF LOW-FREQUENCY OSCILLATION OF SPSC

4.1 *Characteristics of low-frequency oscillation of SPSC and its significance test*

In spring, warm and humid airflow from the ocean meets over Southern China with the cold air from the mid-latitudes. At the lower level of the troposphere, Southern China is located downstream of the velocity center of a powerful southwesterly wind at the southeast side of the Tibetan Plateau, which is marked with intense convergence of wind speed and water vapor and significant precipitation[3-4, 10, 14, 16]. Persistent precipitation happens when fronts move slowly or even stagnate to give rise to active and break phases of the rain, or, oscillations on the intraseasonal scale. As shown in the analysis above, the intraseasonal oscillation also exists in the climatological mean state. As shown in Wang and Xu[19], although the CISO shows large interannual variations, it also has significant similarity from year to year, which presents itself as CISO.

The DB16 wavelet is used to reconstruct the series of daily rainfall in spring for each of the stations. First, the variance ratios between six components of different time scales and primitive series are determined through wavelet reconstruction and Fig.4 gives their zonal distribution. The variance ratio of the annual cycle component is 0.3 to 0.8 and the variance of the d3 component is about 0.1 to 0.2. At 24°-30°N, the annual cycle component is around 0.3 while the CISO is 0.5-0.6. In other words, the CISO is quite important for the precipitation of that region.

Figure 5 gives the time-latitude evolution of the CISO component and the annual cycle component of the

daily rainfall averaged over 110°-120°E. The latter component shows characteristics of increasing with time though with different progression depending on the latitude. For the area 24°-30°N, it is already 4-5 mm in early March before growing slowly afterwards till the end of April and early May when it is 4-5 mm, or, increasing by 2-3 mm during the time. For the former component, there are five processes of oscillation from March to May but with periods of varying length. The value of the oscillation peak (valley) is corresponding to the time of significant rainfall increase (decrease) to be between 1 and 2 mm, or by an oscillatory amplitude of 2-3 mm. From mid-March to early May, the center of oscillation migrates to the south along with the center of precipitation.

To better illustrate the evolution of individual CISO processes and test their significance, the latitude-time evolution is presented in Fig.6 for the difference between the wavelet energy spectrum and the testing thresholds, and the index of the sign of the dominant anomaly, averaged at 110°-120°E. It is seen that the first and second oscillatory processes are the most significant. For the first oscillation, the first half of March is in a dry phase but the second half in a wet phase with the significant zone of oscillation being in 25°-32°N. The centers of the dry and wet phase are of a dual-peak pattern, with the value of the dry phase being around March 11 in 24.5°-27°N and that of the wet phase around March 22 in 28°-32°N, which meets the criteria of a singular point for a wet phase. For the sec ond oscillation, the dry phase appears in April 1-6 that peaks around April 4 in the area around 29°N, and the west phase occurs in April 7-14 that peaks around April 10 in the area of 25.5°-30°N, which also meets the criteria of a singular point of a wet phase. It is now clear that the CISO, as an important composition of the SP-SC, has its peak (valley) value corresponding to the time of significant rainfall increase (decrease), regulat-

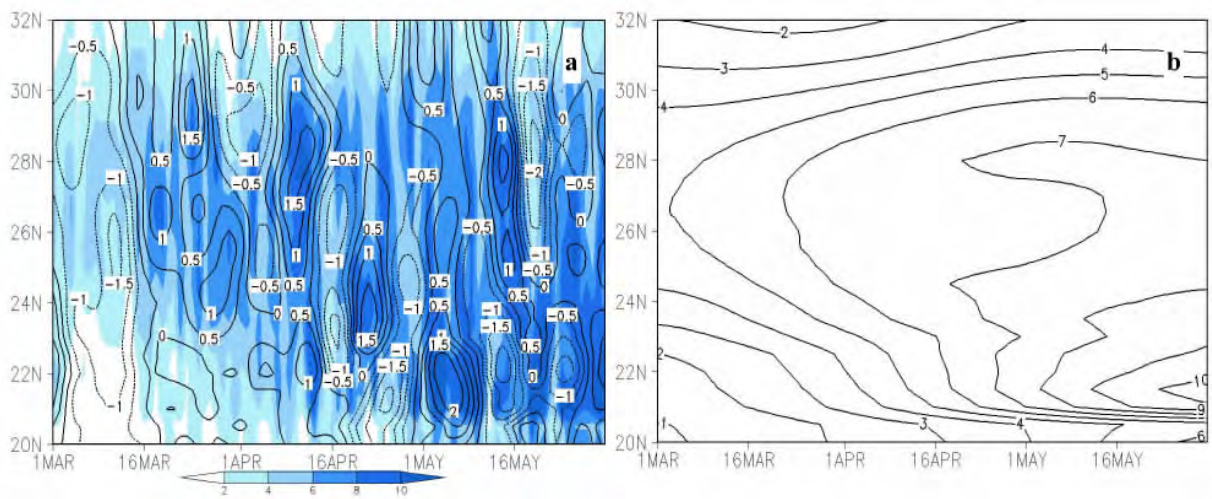

Figure 5. Latitude-time evolution of (a) daily rainfall (shading) and CISO component (contours) averaged over 110°-120°E and (b) the annual cycle component. Units: mm.

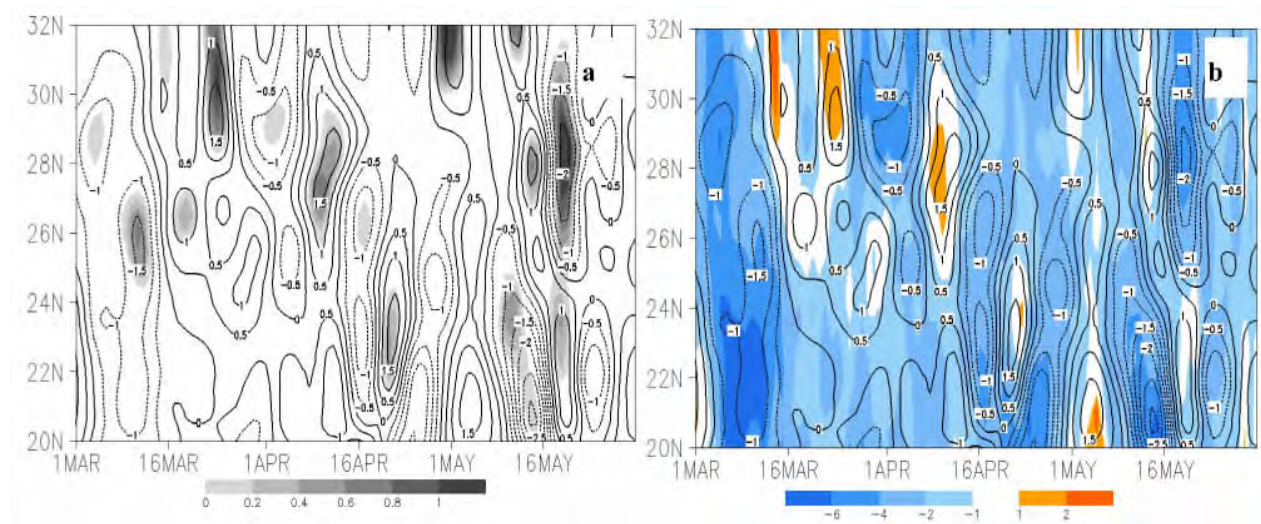

Figure 6. Latitude-time evolution of (a) the CISO component of daily rainfall averaged over 110°-120°E (contours, units: mm) and the difference between the wavelet energy spectrum of CISO and its standard (shadings) and (b) the index for the dominant anomaly sign (shadings, units: year).

ing the evolution of spring precipitation. It is just because of the regulation of CISO that there are two periods of rainfall growth from late March to mid-April.

4.2 *Characteristics of low-frequency oscillation in the general circulation*

Does such statistically significant CISO found in the SPSC have kinematic features coordinated with itself? For this purpose, the atmospheric circulation associated with it will be studied. First, Rain for Southern China, or, RSP, which is an index for the mean SPSC, is defined to be a CISO component of the mean rainfall for the central area (110°-120°E, 23°-30°N) to represent the evolution of CISO within it. The coefficients determined of the correlation between the RSP and the CISO series for individual stations all meet the criteria of the 5% significance level (figure omitted), showing that the series is quite representative. Then, the vectors and coefficients are separately derived of the correlation between the RSP and CISO components for the wind, temperature, divergence and vorticity at 850 hPa, as well as the wind and divergence at 200 hPa.

In the lower troposphere (850 hPa), a pattern of circulation that is favorable for the wet phase of the SPSC is so distributed that it is cyclonic in Eastern China to Japan with the southwesterly and northeasterly prevailing in the southern part of Southern China and the area north of the Yangtze River. They meet over Southern China to form an area of significant convergence with the center over Southwestern China, conducive to the development of ascending motion. In contrast, anti-cyclonic circulation is present over the South China Sea and the central and western Pacific. There are two significant cross-equatorial southerly flows in the equatorial western Pacific; one of them reaches the southern part of Southern China via the South China Sea to meet with the westerly flow coming from the southern side of the Tibetan Plateau to form a field of southwesterly wind in this part of Southern China, and the other heads towards waters east off the Philippines before diverting to become a southwesterly east off the island of Taiwan to contribute jointly to a southwesterly flow south of the cyclonic circulation (Fig.7a). A centre of positive vorticity is present in Southern China while significantly negative vorticity is found in the northeastern part of South China Sea (figure omitted). In addition, the RSP is in significant negative correlation with the temperature in an area of easterly to northeasterly wind north of Southern China but in significant positive correlation with the temperature in an area of southerly over the western North Pacific and South China Sea (figure omitted).

At the upper troposphere (200 hPa), related vectors are reverse-phased with the lower level so that an an ti-cyclonic circulation is distributed over the area from Eastern China to the Okhotsk Sea while a cyclonic circulation is situated over the area from the South China Sea to the central and western Pacific. In Southern China, which is between the two, the easterly and north easterly winds prevail. Airflows are divergent in the east of China with the center of divergence in the area north of Southern China. The effect of dynamic sucking helps develop ascending motion. Significant convergence of airflows exists on the northwestern Philippines, conducive to the formation of descending motion (Fig.7b).

As shown in the analysis above, when low-level airflows converge in the southwest of China but high-level ones diverge in the core of the SPSC and areas to its north, the resultant kinematic effect is conducive to the development of ascending motion in Southern China and turns it into the west phase of CISO. At that time, the subtropical high in SCS is usually westward extended and stronger than normal and cold air is active north of the SPSC core. Therefore, how they evolve in coordination during the evolution of CISO will be studied in more detail in the following

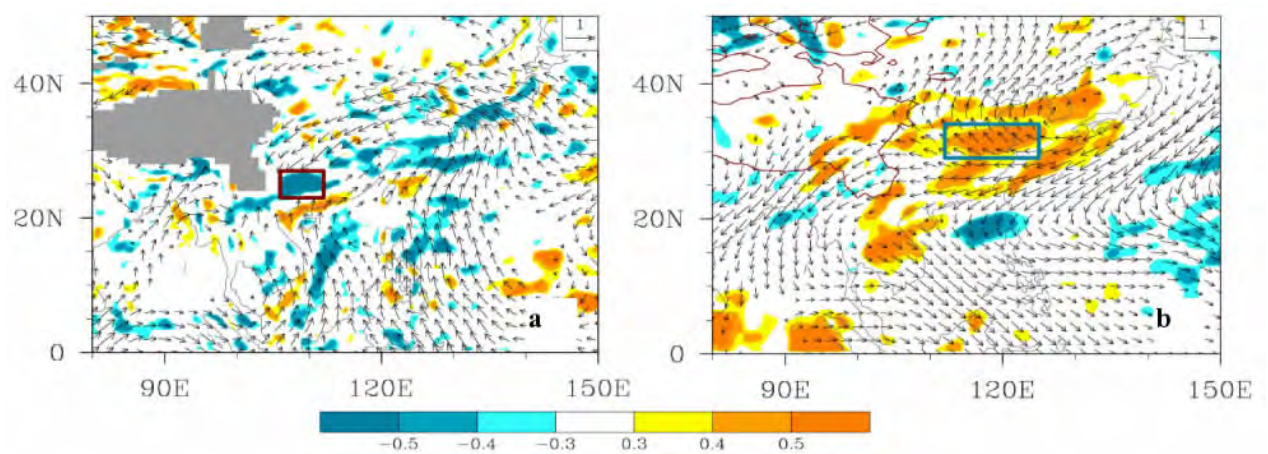

Figure 7. Correlation vectors (vectors) between the RSP and 850-hPa (a) and 200-hPa (b) winds and correlation coefficients of the divergence (shadings). They all surpass the 5% significance test. a: the rectangular domain to the southeast of the plateau (106°-112°E, 23°-27°N) is the one chosen for DIV_WSW. b: the rectangular domain to the north of Southern China (112°-125°E, 29°-34°N) is the one chosen for DIV_NC. The grey shadings in (a) and domain encircled by a red curve in (b) indicate the terrain more than 1 500 m in altitude.

text.

Based on the position of the centers of divergence at both upper and low levels (Fig.7) and the distribution of the correlation coefficient between the temperature field and vorticity at 850 hPa (figure omitted), the CISO components of the following four physical quantities are derived individually: (1) 850-hPa vorticity (*HC_SCS*) averaged over the ridge area of a westward-extended subtropical high in SCS (112°-118°E, 17°-21°N), (2) divergence (*DIV*_WSV) averaged over the area of the Southwest China vorticity (106°-112°E, 23°-27°N), temperature (*Tn*) averaged over the area north of Southern China (107°-117°E, 29°-38°N), and 200-hPa divergence (*DIV*_NC) averaged over the area north of Southern China (112°-125°E, 29°-34°N).

Table 2 gives the correlation coefficients between the RSP and the four physical quantities above and corresponding degree of effective freedom and testing standards. The correlation between them is all significant. The RSP is positively correlated with *DIV*_NC but negatively correlated with the other three physical quantities. Fig.8 presents the curves of their day-to-day evolution in spring. As shown in Fig.8a, the divergence varies in reverse phase between the upper and low level; when the upper level diverges and low level converges, the RSP is in the wet phase. As shown in Fig.8b, when the westward-extended ridge of the subtropical high of SCS is relatively strong and the area north of Southern China is affected by cold air, the RSP is in the wet phase. The RSP is in the dry phase otherwise.

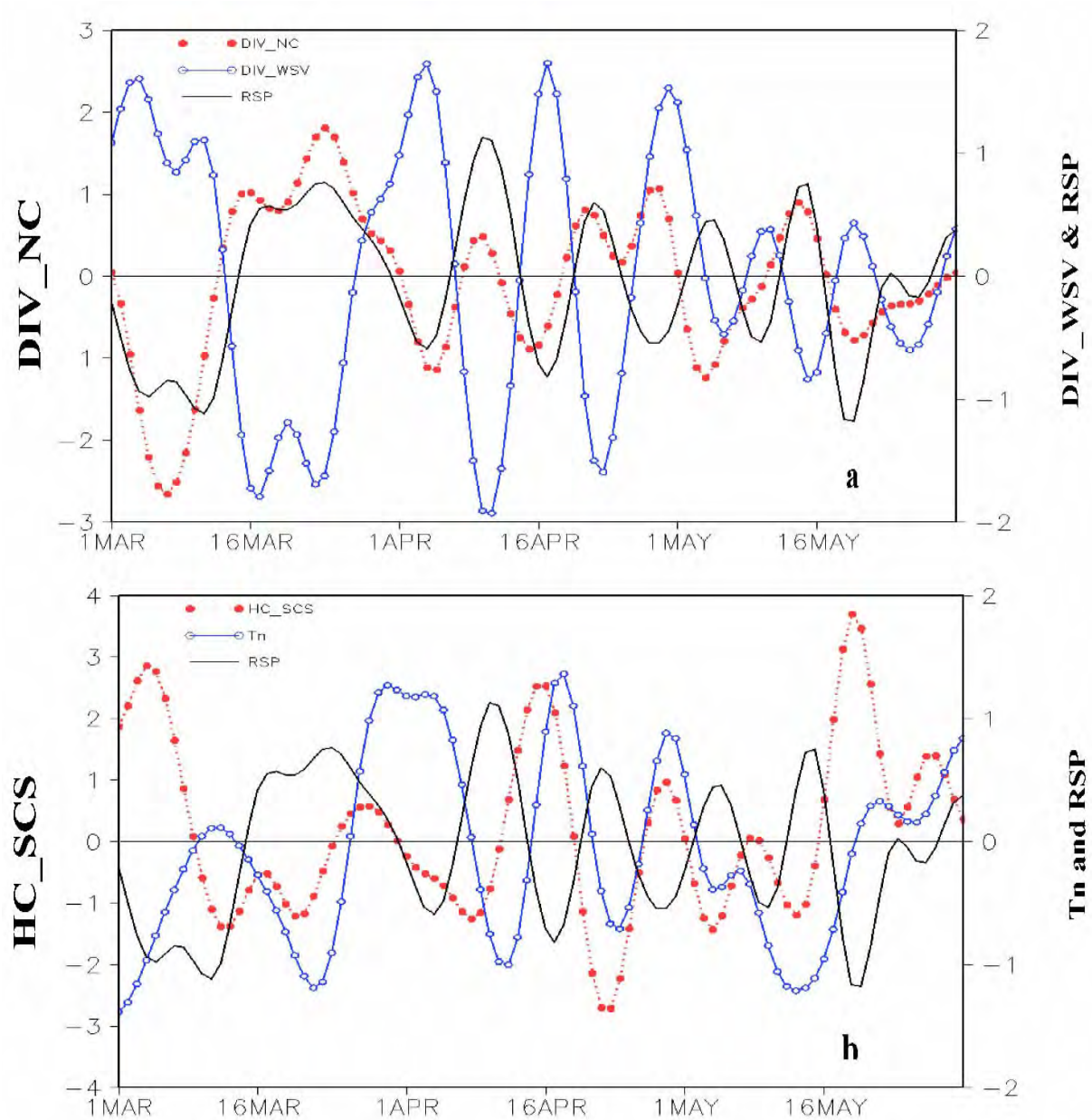

Figure 8. Daily evolution in spring of the RSP and individual physical quantities of the CISO component. a: RSP (unit: mm), *DIV*_NC (unit: 10^{-6} s^{-1}), *DIV*_WSV (10^{-6} s^{-1}); b: RSP (same as in a), *Tn* (unit:℃), *HC*_SCS (10^{-6} s^{-1}).

As shown in the analysis above, the CISO of SPSC is not only significant statistically but also corresponds to coordinated allocation of the atmospheric circulation: When CISO is jointly affected by synoptic systems from the mid- and higher-latitude and extra-tropics, the east of China is marked by cyclonic circulation in lower troposphere and anti-cyclonic circulation in upper troposphere. Because of the allocated circulation of baroclinic structure of low-level convergence associated with high-level divergence, ascending motion is set free in Southern China where the wet phase of CISO prevails.

Table 2. Correlation coefficients between RSP and *DIV*_NC, *DIV*_WSV, *JC*_SCS and *Tn*.

	RSP & *DIV*_NC	RSP & *DIV*_SWV	RSP & HC_SCS	RSP & *Tn*
Correl. coeff.	0.64	-0.79	-0.52	-0.31
Degree of effective freedom	55	53	59	56
Standard of 5% significance test	0.27	0.27	0.25	0.27

5 SUMMARY AND DISCUSSION

(1) Two of the SPSC large-value centers are located in Fogang and Qingyuan, south of the Nanling Mountains, and Wuyi Mountains, and areas of relatively small amount of rain are present in the southwestern Jiangxi and southern Hunan. Such distribution results from the effect of rain enhancement due to orographic uplifting and that of rain reduction caused by leeward slopes. With the increase of rain amount with time, the rain season begins in various parts of Southern China from Pentad 12 to 24. It first starts from the large-value centers and then progresses to the surrounding areas. After Pentad 20, the rain season is well into its prime period everywhere.

(2) Being an important component of SPSC, the CISO is not only significant statistically, but also corresponding to coordinated allocation of the atmospheric circulation. The value of the oscillatory peak (valley) corresponds to the time of significant rainfall increase (decrease) that regulates the springtime precipitation. It is just because of the adjustment by CISO that the amount of rain increases from late March to early-to mid-April in Southern China. The CISO is jointly affected by synoptic systems from the mid- and higher-latitudes as well as the extra-tropics. When lower tropospheric circulation is cyclonic and upper tropospheric circulation is anti-cyclonic in the east of China, the CISO is in the wet phase as Southern China is influenced by a baroclinic structure of lower-level convergence versus upper-level divergence.

(3) The CISO reflects the similarity of ISO from year to year thought the latter varies much between dif ferent years. Then, what is the significant ISO period of the SPSC? And what are the characteristics and mechanisms of oscillations in components with different peri ods? They should be explored further.

Acknowledgement: The authors would like to express their gratitude towards the Center of Meteorological Information, China for its observations of daily rainfall and the European Center for Medium-Range Weather Forecasting for the ER-A-Interim reanalysis data.

REFERENCES:

[1] GAO You-xi, XU Shu-ying, GUO Qi-yun, et al. The Monsoon Regions and Regional Climate of China [M]// A Number of Issues with the East Asian Monsoons. Beijing: Science Press, 1962.
[2] BAO Cheng-lan. Synoptics on the Tropics [M]. Beijing: Science Press, 1980.
[3] TIAN S F, YASUNARI T. Climatological aspects and mechanism of spring persistent rains over central China [J]. J Meteorol Soc Japan, 1998, 76(1): 57-71.
[4] CHEN Lun-xun, LI Wei, ZHAO Ping, et al. On the Process of Summer Monsoon Onset over East Asia [J]. Clim Environ Res, 2000, 5(4): 345-355.
[5] LIANG Jian-yin, WU Shang-sen. Formation reasons of drought and flood in the rain season of Guangdong and preceding impact factors [J]. J Trop Meteorol, 2001, 17(2): 97-108.
[6] WANG H J, XUE F, ZHOU G Q. The spring monsoon in south China and its relationship to large-scale circulation features [J]. Adv Atmos Sci, 2002, 19(4): 651-664.
[7] QIAN W H, KANG H S, LEE D K. Distribution of seasonal rainfall in the East Asian monsoon region [J]. Theor Appl Climatol, 2002, 73(3): 151-168.
[8] WANG B, LinHo. Rainy season of the Asian-Pacific summer monsoon [J]. J Climate, 2002, 15(4): 386-398.
[9] CHI Yan-zhen. Characteristics of precipitation in the annually first rainy season in South China and their interaction with the summer monsoon in the South China Sea [D]. Nanjing: Nanjing University of Information Engineering, 2005.
[10] WAN Ri-jin, WU Guo-xiong. On the mechanism for climatic causation of spring precipitation in the area south of Yangtze River [J]. Sci China (Ser D Earth Sci), 2006. 36(1): 936-950.
[11] ZHAO P, ZHANG R H, LIU J P, et al. Onset of southwesterly wind over eastern China and associated atmospheric circulation and rainfall [J]. Clim Dyn, 2007, 28 (7): 797-811.
[12] WANG Zun-ya, DING Yi-hui. Climatic characteristics of rainy seasons in China [J]. Chin J Atmos Sci, 2008, 32 (1): 1-10.
[13] WAN Ri-jin, WU Guo-xiong. Temporal and spatial distribution of the spring persistent rains over southeastern China [J]. Acta Meteorol Sinica, 2008, 66(3): 310-319.
[14] WAN Ri-jin, WANG Tong-mei, WU Guo-xiong. Tempo-

ral variations of the spring persistent rains and SCS subtropical high and their correlations to the circulation and precipitation of the East Asia summer monsoon [J]. Acta Meteorol Sinica, 2008, 66(5): 800-807.
[15] HE Jin-hai, ZHAO Ping, ZHU Cong-wen, et al. Discussions on the East Asian subtropical monsoon [J]. Acta Meteorol Sinica, 2008, 66(5): 683-696.
[16] LinHo L H, HUANG X L, LAU N C. Winter-to-spring transition in East Asia: A planetary-scale perspective of the South China spring rain onset [J]. J Climate, 2008, 21 (13): 3 081-3 096.
[17] ZHU Cong-wen, ZHOU Xiu-ji, ZHAO Ping, et al. Onset of East Asian subtropical summer monsoon and rainy season in China [J]. Sci China Earth Sci, 2011, doi: 10.1007/s11430-011-4284-0.
[18] NAKAZAWA T. Seasonal phase lock of intraseasonal variation during the Asian summer monsoon [J]. J Meteorol Soc Japan, 1992, 70: 597-611.
[19] WANG B, Xu X H. Northern Hemisphere Summer Monsoon Singularities and Climatological Intraseasonal Oscillation[J]. J Climate, 1997, 10(5): 1 071-1 085.
[20] DEE D P, UPPALA S M, SIMMONS A J, et al. The ERA-Interim reanalysis: configuration and performance of the data assimilation system [J]. Quart J Roy Meteorol Soc, 2011, 137: 553-597.
[21] TORRENCE C, COMPO G P. A practical guide to wavelet analysis [J]. Bull Amer Meteorol Soc, 1998, 79 (1): 61-78.
[22] COHEN A, DAUBECHIES I, FEAUVEAU J C. Biorthogonal bases of compactly supported wavelets [J]. Comm Pure Appl Math, 1992, 45: 485-560.
[23] ROBERT E. LIVEZEY, CHEN W Y. Statistical field significance and its determination by Monte Carlo technique [J]. Mon Wea Rev, 1983, 111(1): 46-59.
[24] TU Qi-pu, WANG Jun-de, DING Yu-guo, et al. Statistics of Applied Probability for Meteorology [M]. Beijing: China Meteorological Press, 1984: 32-34.
[25] CHEN W Y. Fluctuations in Northern Hemisphere 700 mb height field associated with Southern Oscillation [J]. Mon Wea Rev, 1982, 110(7): 808-883.
[26] WEN Min, ZHANG Ren-he. Possible mechanisms for maintaining atmospheric quasi-biweekly oscillation near Sumatra [J]. Chin Sci Bull, 2005, 50(9): 938-940.
[27] SMITH R B. The influence of mountains on the atmosphere [J]. Adv Geophys, 1979, 29: 87-230.
[28] LIN Zhi-guang. Climatology on Orographic Precipiation [M]. Beijing: Science Press, 1995: 96-105.

Citation: PAN Wei-juan, LI Chun-hui and JIANG Cheng-lin. Climatological characteristics of spring precipitation over southern China and its intraseasonal oscillation [J]. J Trop Meteorol, 2016, 22(2): 233-242.